



Direct contact membrane distillation – a potential technology for treating saline water in Quang Dien and Phu Vang district, Thua Thien Hue province

Ve Quoc Linh^{*}, Do Minh Cuong¹, Nguyen Thanh Cuong¹, Nguyen Quoc Huy¹,
Phan Ton Thanh Tam¹, Nguyen Quang Lich²

¹ Faculty of Engineering and Food Technology, University of Agriculture and Forestry, Hue University,
Thua Thien Hue 530000, Vietnam

² School of Engineering and Technology, Hue University, Thua Thien Hue 530000, Vietnam

Abstract. This study aims to clarify the salinization degree of irrigation water in Quang Dien and Phu Vang districts in Winter-Spring crop season and to propose a potential technology to treat saline water on lab-scale. The majority of irrigation water was brackish water (70%) at Quang Phuoc, Quang Loi, and Phu Dien villages with water concentration of up to nearly 7.1‰. For Quang Thai and Phu An villages, the salinization degree is much lower when the percentage of brackish water was from 30% to 40%. Direct contact membrane distillation (DCMD) was implemented to treat 20‰ - 40‰ concentrations of saline water. The experimental results revealed that the freshwater production by DCMD met the requirements of irrigation water when the salinity was under 0.1‰. Additionally, feed inlet temperature was the most effective factor to produce the highest amount of freshwater compared to volume flowrate and feed concentration factors.

Keywords: Direct contact membrane distillation, Quang Dien, Phu Vang, DCMD efficiency

1 Introduction

Salinization is the process of seawater penetrating inland, causing ponds, lakes, and underground water sources to become contaminated with salt. The higher the amount of salt in the water is, the lower the implementation of water for irrigation purposes is. The classification of saline water is in Table 1.

The process of salinization in Thua Thien Hue takes place mainly in the depressions, adjacent to the Tam Giang - Cau Hai lagoon system and the Thuan An - Tu Hien estuary. The salinization process causes negative consequences for agricultural production and the ecological environment in depressions along the Huong and Bo rivers. The total affected area is estimated at about 2,000-2,500 hectares [5]. Because the average rainfall from the beginning of 2020 until now has been lower than the average for many years and is unevenly distributed, many irrigation and hydropower reservoirs in Thua Thien Hue province are always in a "thirsty" state [6]. Dozens of hectares of local rice died due to salinization and thousands of hectares lacked water until the

** Corresponding: vqlinh@hueuni.edu.vn*

end of the Winter-Spring crop season. According to the Department of Agriculture and Rural Development of Thua Thien Hue province, the area of rice died due to salinization was 79.8 hectares in 2020, mainly in the communes of Phu Da, Phu Dien, Vinh Xuan, Vinh Ha, Phu Gia, Phu Xuan (Phu Vang district); Quang Cong commune (Quang Dien district); Hai Duong and Huong Phong communes (Huong Tra town); Loc Tri and Vinh Hung communes (Phu Loc district) [6].

Table 1. Water salinity separation level, modified from [1-4]

| Order | Water type | Salinity level | ‰ | Notes |
|-------|----------------|---|------------|--|
| 1 | Freshwater | Freshwater (for drinking water in Viet Nam) | 0.25 – 0.3 | Typical irrigation water salinity: < 0.35‰ |
| | | Brackish freshwater | 0.3 - 1 | 0.350‰ – 0.5‰: limit irrigation |
| 2 | Brackish water | Mildly | 1 - 5 | > 0.5‰: stop irrigating |
| | | Moderately | 5 - 15 | |
| | | Heavily | 15 - 35 | |
| 3 | Seawater | Normal seawater | 35 - 50 | |
| 4 | Brine | | > 50 | |
| 5 | Dead sea | | 330 | |

Data from 2013 to 2017 revealed that the salinization process occurred more and more severely, especially in 2014 in Quang Dien district. Annually, the May-August duration obtained the highest salinization level due to the higher temperature and lack of rainfall [5]. The effects of salinization in Quang Dien district are mainly on the production land agriculture, especially paddy fields. According to statistics, in 2014 the total area for paddy was 4,503.7 hectares, of which 530 hectares were affected by salinization, accounting for 11.8% of the total paddy area [7]. According to [5], the salinity of water for irrigation purposes ranged from 2.1‰ – 14.3‰ and 1.3‰ - 14.8‰ at Quang Phuoc and Quang Loi villages, respectively in 2018 Summer-Autumn crop season. Additionally, the irrigation water in Quang Thai village also obtained high salinity with the range of (0.009‰ - 9‰) and of (2.37‰ - 29‰) for 2021 Winter-Spring crop season and 2021 Summer-Autumn crop season, respectively [8]. The phenomenon of salinization process occurred in the dry season due to lack of rainfall in Phu Vang district. Most villages in the Phu Vang district could only produce one Winter-Spring crop season. According to [9], the irrigation water in Phu Dien and Vinh Xuan villages ranged from mildly brackish water (29%-30% of the total sampling waters) to moderately brackish water (69%-70% of the total sampling waters), and the salinity of water reached up to 14.8‰ at Ke Sung hamlet and 13.9‰ at Xuan Thien Thuong hamlet in 2018 Winter-Spring crop season. Regarding Table 1, the treatment of saline water for irrigation purposes in Quang Dien and Phu Vang districts is an urgent task.

Desalination could be one of the potential technologies to meet this task requirement. This technique could be implemented to treat water having a very low concentration or much higher concentration of dissolved salt [10]. Freshwater could be achieved by thermal process (multi-effect desalination or multistage flashing) or membrane methods (reverse osmosis). Compared to membrane distillation (MD) technology, reverse osmosis (RO) doesn't need to use thermal energy to treat saline water, however, RO uses much more electrical energy to produce freshwater. It is estimated that electrical consumption for RO is from 3 kWh/m³ to 7 kWh/m³, whereas MD only uses from 0.6 kWh/m³ to 1.8 kWh/m³ [11-14]. The requirements of operating conditions for RO like high-quality feedwater, high applied pressure, and inability of high-concentration solution treatment were also disadvantages of this technology. Membrane distillation was a technique that combined both thermal and membrane processes to treat saline water [15, 16]. The disadvantage of consuming much energy for MD to treat saline water can be lessened by implementing renewable energy or low-grade waste heat [17-20] because MD can be operated at lower temperatures (under boiling temperature) and pressure compared with conventional distillation and pressure-driven membrane separation technologies like RO [19, 21-23]. As estimated by Choi et al. [24], the water cost of MD was higher than that of RO and RO-MD. This is due to the cost of thermal energy, and this cost could be reduced by implementing alternative energy sources instead of using electrical energy. Consequently, the MD system also has economic feasibility if the thermal energy cost is reduced. Moreover, operating MD system without high hydrostatic pressure can reduce investment costs when inexpensive non-corrosive materials can be used to make the MD [25]. The membrane fouling in MD process was also much less than that in RO or nanofiltration (NF) due to lacking high hydrostatic pressure at the operating stage [25]. Therefore, MD system can be sustainably operated with little pre-treatment of seawater without any membrane fouling problems [25]. Although large-scale commercialization is also an obstacle hindering the development of MD, however, some lab-scale and pilot-scale studies showed that MD is a potential and promising technology for saline water treatment and other niche applications [26]. Basically, MD consists of four configurations: direct contact membrane distillation (DCMD), vacuum membrane distillation (VMD), air gap membrane distillation (AGMD), and sweeping gas membrane distillation (SGMD) [27]. Additionally, there were two more hybrid configurations: thermostatic sweeping gas membrane distillation (TSGMD) and liquid gap membrane distillation (LGMD) [28, 29]. Amongst four MD configurations, DCMD was studied the most in the academic field because of its benefits: the simplest configuration, high saline concentration treatment with up to 70‰, operating at atmospheric pressure and low temperature [10, 21, 23, 30, 31].

In the present work, the current state of salinization process in Winter-Spring crop season happening in Quang Dien and Phu Vang district is studied. Based on that, the simulated saline water was prepared in lab scale to examine the treatment capability and the efficiency of DCMD technology under the effect of feed inlet temperature, volume flow rate, and feed concentration.

A much higher saline feed water of up to 40‰ (higher than salinity of normal seawater) was used in this study.

2 Theory

2.1 Heat transfer

Heat and mass transfer happen at the same time in direct contact membrane distillation. For heat transfer, there are three continuous stages as following mention: the movement of convective heat to the feed membrane through the liquid boundary layer (Q_i); the heat transport through membrane pores in form of conduction heat and vapour latent heat (Q_m); and the removal of convective heat from permeate membrane surface to the liquid boundary layer (Q_p). At steady state, heat transfer in DCMD can be expressed [31]:

$$Q_i = Q_m = Q_p = Q \quad (1)$$

$$h_f \times A \times (T_f - T_{m,f}) = \frac{k_m}{\delta_m} \times A \times (T_{m,f} - T_{m,p}) + J_w \times A \times \Delta H_{v,w} = h_p \times A \times (T_{m,p} - T_p)$$

Or

$$Q = \left[\frac{1}{h_f} + \frac{1}{k_m/\delta_m + J_w \Delta H_{v,w}/(T_{m,f} - T_{m,p})} + \frac{1}{h_p} \right]^{-1} \times (T_f - T_p) \quad (2)$$

$$Q = H \times \Delta T$$

The Maxwell (Type II) model proposed in previous studies [32, 33] was used to calculate the thermal conductivity of membrane (k_m)

$$k_m = \frac{k_g [1 + 2\beta\varphi + (2\beta^3 - 0.1\beta)\varphi^2 + 0.05\varphi^3 \exp(4.5\beta)]}{1 - \beta\varphi} \quad (3)$$

$$\beta = (k_p - k_g)/(k_p + 2k_g); \varphi = 1 - \varepsilon_m$$

From Equation (1), The membrane surface temperature at feed and permeate side can be derived:

$$T_{m,f} = \frac{h_m \left(T_p + \frac{h_f}{h_p} T_f \right) + h_f T_f - J_w \Delta H_{v,w}}{h_m + h_f \left(1 + \frac{h_m}{h_p} \right)} \quad (4)$$

$$T_{m,p} = \frac{h_m \left(T_f + \frac{h_p}{h_f} T_p \right) + h_p T_p + J_w \Delta H_{v,w}}{h_m + h_p \left(1 + \frac{h_m}{h_f} \right)} \quad (5)$$

2.2 Mass transfer in DCMD

The mass transfer in DCMD process can be expressed [23, 34-37]:

$$J_w = C_m (p_{v,sf} - p_{v,sp}) \quad (6)$$

The Antoine and Sharqawy's equations [31, 36, 38] were applied to estimate the partial pressures of water vapour. The membrane permeability coefficient (C_m) proposed by Ding et al. [39] was implemented in this study.

$$C_m = \frac{1}{RT_m \delta_m} \left[\left(\frac{3\tau}{2\varepsilon_m r} \left(\frac{\pi M}{8RT_m} \right)^{1/2} + \frac{p_a \tau}{\varepsilon_m PD} \right)^{-1} + 0.125 \frac{\varepsilon_m r^2 M P_m}{\tau \mu} \right] \quad (7)$$

If saline water was used in feed side, the concentration factor should be considered in predicting mass flux. To reveal the relationship between mass flux and concentration polarization effect, the following expression was applied [40, 41].

$$J_w = \rho_f k_s \ln \left(\frac{S_{m,f}}{S_f} \right) \quad (8)$$

Where mass transfer coefficient through boundary layer, k_s ($m.s^{-1}$) was determined [42]:

$$k_s = \frac{D}{\delta} \quad (9)$$

Where (δ) (m) was the boundary layer thickness, and D ($m^2.s^{-1}$) was the solute diffusion coefficient [42, 43].

$$\delta = \frac{5 \times d_h}{\sqrt{Re_f}} \quad (10)$$

$$D = (0.72598 + 0.023087 \times T_{m,f} + 0.00027657 \times T_{m,f}^2) \times 10^{-9} \quad (11)$$

3 Experimental set up

The water samples taken to measure salinity are water used for irrigation. The locations chosen to take water samples for salinity analysis are areas adjacent to the lagoon system. Three different

villages (Quang Phuoc, Quang Loi, and Quang Thai) in Quang Dien district and two various villages (Phu Dien, and Phu An) in Phu Vang district were chosen for taking water samples. The locations and the coordinates for taking water samples to measure salinity were described in Table DS1, Table DS2, Table DS3, Table DS4, Table DS5 (Data set file). At each village, salinity of 10 different water samples were measured by water quality tester C-100 multifunctional 5 in 1 seawater test pen, which was manufactured by TOPINCN, China. At each sampling point, water samples were measured repeatedly 3 times to ensure data accuracy. The coordinates of the sampling point were recorded using google map app.

Based on the current salinization of irrigation water in Quang Dien and Phu Vang districts, a feed solution with concentration of 20‰ and 40‰ was prepared in laboratory. To investigate the treatment efficiency of saline water, a DCMD module with 4mm-height channel was fabricated. A 0.45µm commercially PTFE membrane with 225 cm² effective area was used in this experiment. The hot urn (model BE-25L-T of 2500 W) equipped with temperature controller was used to heat the feed solution up to necessary temperature. A combination between the chiller (model CW-5000) and heat exchanger was implemented to cool down the permeate solution at fixed temperature. Both feed and permeate solutions were pumped counter-currently. To measure the temperatures and volume flowrate at both sides of the DCMD modules, four probe temperature sensors WZP - PT100 and two water flowmeter sensors (YF-S201) being from YANHAO, China were applied. All the measured data were collected by DI-2108 data logger. The experimental process for saline water treatment by DCMD technology was illustrated in Fig. 1.

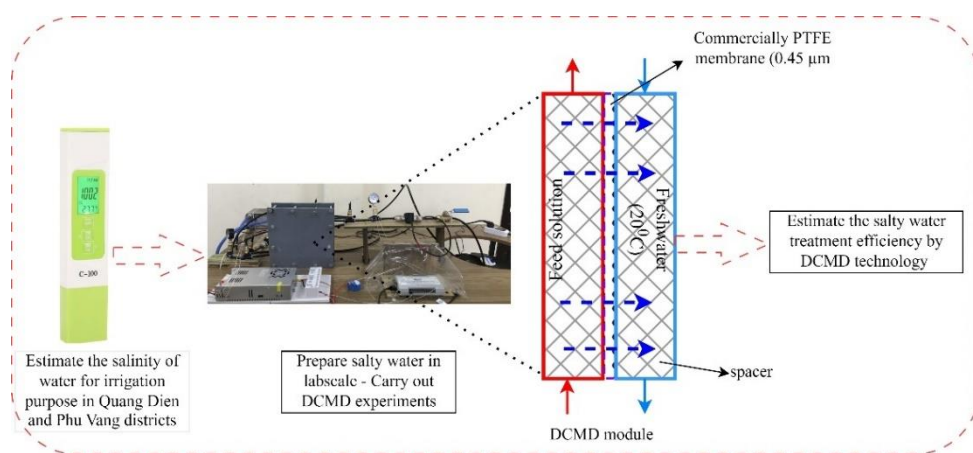


Fig. 1. Experimental process for treating saline water by DCMD technology in lab scale

The feed inlet temperature ranged from 40°C to 50°C, whereas 20°C was the temperature of permeate inlet temperature for all experimental runs. The equal volume flowrates were

adjusted at both sides with 1 L/min and 1.8 L/min. The feed concentration ranged from 20‰ and 40‰ in lab-scale. Each experimental case was described in Table 2.

Table 2. Experimental conditions for investigating the treatment capability of DCMD

| Experimental No. | Experimental conditions |
|------------------|--|
| 1 | ($T_{fi} = 40^{\circ}\text{C}$; $V_f = V_p = 1.8 \text{ L/min}$; $T_{pi} = 20^{\circ}\text{C}$; $S_f = 20\text{‰}$) |
| | ($T_{fi} = 45^{\circ}\text{C}$; $V_f = V_p = 1.8 \text{ L/min}$; $T_{pi} = 20^{\circ}\text{C}$; $S_f = 20\text{‰}$) |
| | ($T_{fi} = 50^{\circ}\text{C}$; $V_f = V_p = 1.8 \text{ L/min}$; $T_{pi} = 20^{\circ}\text{C}$; $S_f = 20\text{‰}$) |
| 2 | ($T_{fi} = 50^{\circ}\text{C}$; $V_f = V_p = 1 \text{ L/min}$; $T_{pi} = 20^{\circ}\text{C}$; $S_f = 20\text{‰}$) |
| | ($T_{fi} = 50^{\circ}\text{C}$; $V_f = V_p = 1.8 \text{ L/min}$; $T_{pi} = 20^{\circ}\text{C}$; $S_f = 20\text{‰}$) |
| 3 | ($T_{fi} = 50^{\circ}\text{C}$; $V_f = V_p = 1.8 \text{ L/min}$; $T_{pi} = 20^{\circ}\text{C}$; $S_f = 20\text{‰}$) |
| | ($T_{fi} = 50^{\circ}\text{C}$; $V_f = V_p = 1.8 \text{ L/min}$; $T_{pi} = 20^{\circ}\text{C}$; $S_f = 40\text{‰}$) |

4 Results and Discussions

4.1 Current salinity level of water source for irrigation in Quang Dien district, Thua Thien Hue province

At Quang Phuoc village, the water samples were taken at Phuoc Lam, Phuoc Ly, Mai Duong, and Phuoc Lap. The water salinity for irrigation ranged from 0.761‰ to 7.99‰. The highest water salinity was at Phuoc Lam and Mai Duong hamlet. According to Table 1, and Fig. 2a, 90% of water samples were brackish water. As mentioned in [5], the water salinity in Quang Phuoc village was higher and up to 14.3‰ in Summer-Autumn crop season. At Quang Loi village, the water samples were taken at Ngu My Thanh, Thuy Lap, Thap Nhuan, Ha Cong, and Ha Lac hamlet. As shown in Fig. 2b, 70% and 30% were for brackish water and brackish freshwater, respectively. Thanh et al. [5] also mentioned that the salinity of water samples was up to 14.8‰ in Summer-Autumn crop season. The reason for the higher water salinity in Summer-Autumn crop season in comparison to Winter-Spring crop season was because of higher ambient temperature when Summer-Autumn crop season lasted from May to September in Thua Thien Hue province.

For Quang Thai village, Trung Kien, Trung Lang, Cua Lac dam, Lai Ha, and Dong Ho hamlet were chosen to measure the water samples. The salinity of water samples ranged from 0.032‰ to 6.23‰, much lower than that at selected locations at Quang Phuoc and Quang Loi hamlet. Brackish water took into account 40%. The rest 60% was for brackish freshwater and freshwater levels, as shown in Fig. 2c. Hai et al. [8] presented that the salinity of water samples in the 2021 Winter-Spring crop season at Quang Thai village ranged from 0.009‰ – 8.999‰, and the 2021 Summer-Autumn crop season also had higher water salinity within the range of (2.37‰ – 29.002‰).

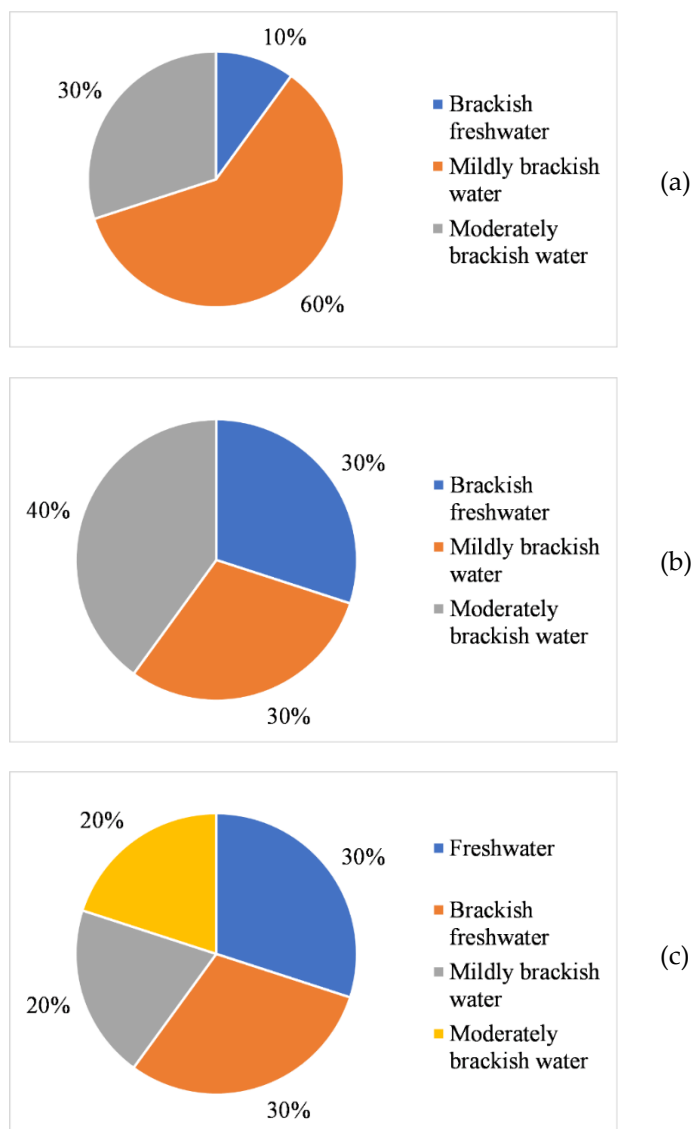


Fig. 2. The current water salinity level for irrigation purposes in Winter-Spring crop season in Quang Dien district; (a) Quang Phuoc; (b) Quang Loi; (c) Quang Thai

According to Table 1, most of the water samples in Quang Dien district had much higher salinity levels than those for irrigation criteria. Therefore, it is necessary to find an efficient treatment method to solve this problem. This technology will be discussed in more detail in section 4.3.

4.2 Current salinity level of water source for irrigation in Phu Vang district, Thua Thien Hue province

At Phu Dien village, most of water samples were taken at two main hamlets: Ke Sung, and My Khanh. According to Fig. 3a, the majority of measured water was brackish water with 70%, and the salinity of water samples was in the range of (0.200‰ – 6.23‰). Thanh [9] also mentioned that 70% and 30% were for moderately brackish water and mildly brackish water, respectively in 2018 Winter-Spring crop season in Phu Dien village. The salinity of irrigation water was much higher in Ke Sung hamlet with 14.8‰ [9]. The broken of clay layer preventing water salinity due to the titanium exploitation was estimated as the initial reason, and most of water irrigation reservoirs at Ke Sung and My Khanh hamlet were next to Ha Trung dam [9].

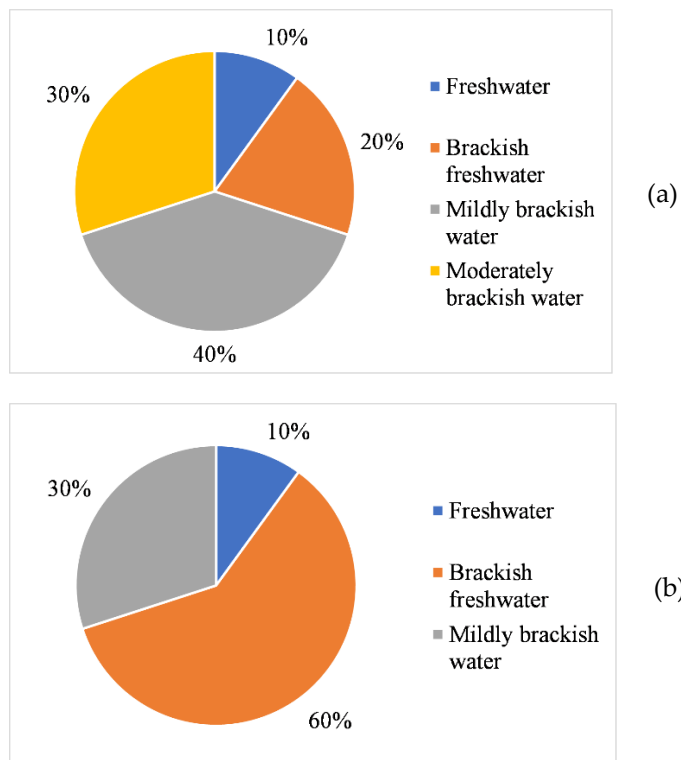


Fig. 3. The current water salinity level for irrigation purposes in Winter-Spring crop season in Phu Vang district; (a) Phu Dien; (b) Phu An

At Phu An village, Thuy Dien, Dong Mieu, Anh Truyen, Trieu Thuy, and Mong An hamlet were selected locations to measure the salinity of irrigation water. The measured values revealed the water samples had much lower salinity than those in Phu Dien village. The salinity of irrigation water ranged from 0.256‰ to 1.5‰, therefore most of water at Phu An village was brackish freshwater with 60%, as shown in Fig. 3b. Based on the geographical location, most of the water reservoirs for irrigation purposes located far from Chuon dam and Sam dam, therefore the salinization process occurred much lower than other investigated locations in this study.

Consequently, there was the salinization process in both Phu Dien and Phu An villages. So, the effective method for decreasing the salinity of water to meet irrigation requirements was necessary, and this technology will be discussed in more detail in section 4.3.

4.3 The potential treatment of DCMD technology for saline water in Thua Thien Hue province

Effect of feed inlet temperature on DCDM efficiency

The experimental conditions were Experimental No.1 shown in Table 2. As can be seen from Fig. 4, the feed inlet temperature significantly affected the measured mass flux [29, 44-46]. In comparison to nearly 8.6 kg/m²-h at 40°C, the mass flux reached up to 16.6 kg/m²-h at 50°C, nearly 94%. The exponential dependence of partial vapour pressure on temperature was the main reason for that increase in mass flux [31, 36].

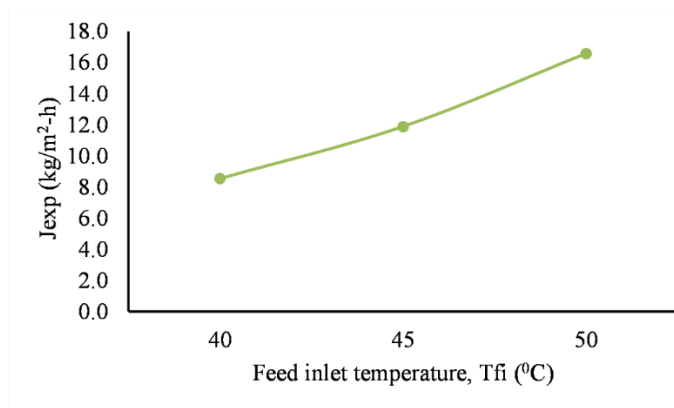


Fig. 4. Permeate flux vs feed inlet temperature

Additionally, the degree of water molecule vaporization rose significantly when the feed inlet temperature went up [47]. This could be reflected through the considerable rise of total heat transfer coefficient (18.1%) compared to the internal heat transfer coefficient (nearly 4%), as showed in Fig. 5. The rise of permeate flux due to temperature was also proved through the drop of thermal boundary layer thickness (nearly 7.6%) and the increase of mass transfer coefficient through boundary layer (nearly 7.1%), as showed in Fig. 6. According to [34, 45], the slight drop of feed solution viscosity and the rise of the diffusion coefficient of solute, as described in Equation (9) contributed to the decrease of boundary layer thickness and the increase of mass transfer coefficient through boundary layer.

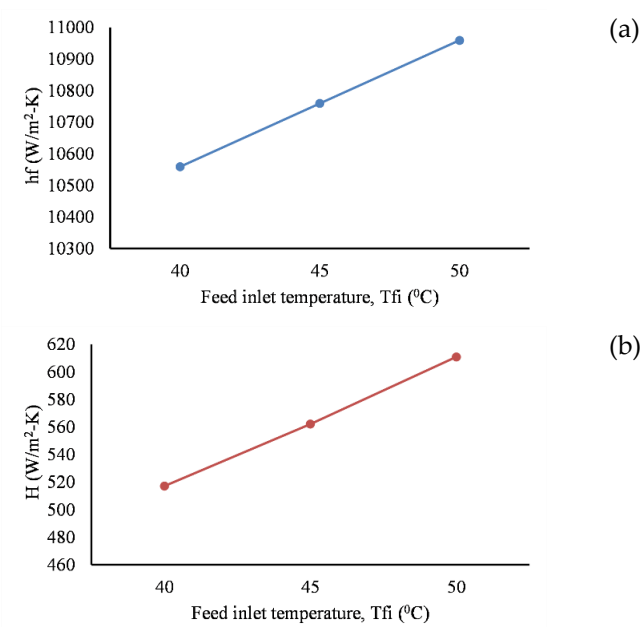


Fig. 5. (a) Internal feed heat transfer coefficient; (b) total heat transfer coefficient vs feed inlet temperature

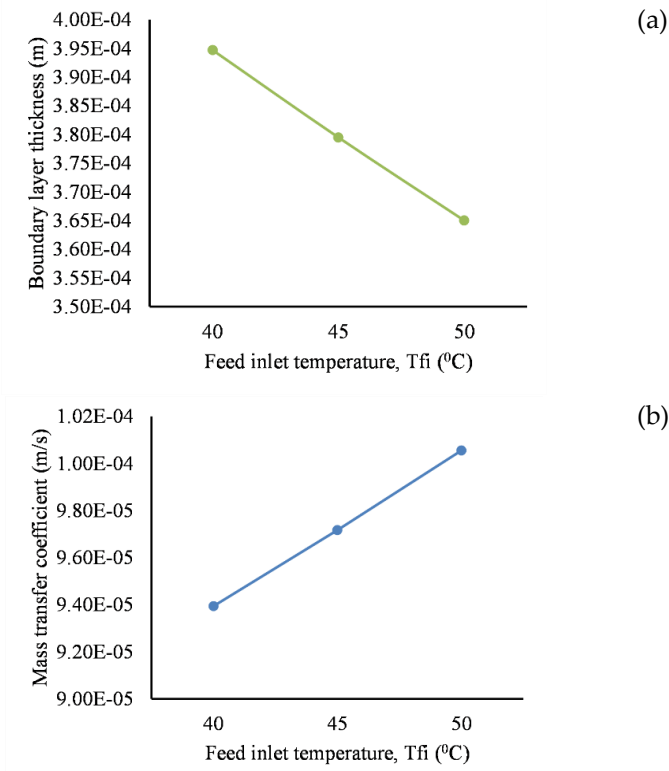


Fig. 6. (a) Boundary layer thickness; (b) Mass transfer coefficient through boundary layer vs feed inlet temperature

Effect of volume flow rate on DCMD efficiency

The operating parameters for this experiment were experimental No.2 showed in Table 2. From Fig. 7, the insignificant increase in mass flux due to the volume flow rate can be attributed to the following reasons. Firstly, the heat of vaporization was only the function of temperature, it was independent on the volume flow rate [23]. This could be clarified through the Fig. 8b where the total heat transfer coefficient increased by 5% at 1.8 L/min compared to at 1 l/min. In fact, the internal heat transfer coefficient at feed side was enhance because of the enhancement of Reynolds number in this case of experiment, as showed in Fig. 8a. Secondly, the increase in volume flow rate caused the significant drop of boundary layer thickness by 25.1%, and that led to the considerable rise in mass transfer coefficient through boundary layer by 37.3%, as mentioned in Fig. 9. Moreover, the membrane surface temperatures reached closer to corresponding bulk temperatures in case of the rise of volume flow rate, and this caused the larger transmembrane temperature difference which led to higher mass flux [31]. As a result, the permeate flux increase by nearly 6% at 1.8 L/min compared to at 1 L/min.

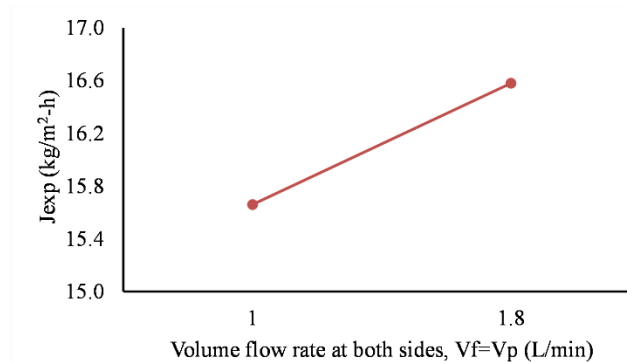


Fig. 7. Permeate flux vs volume flow rate

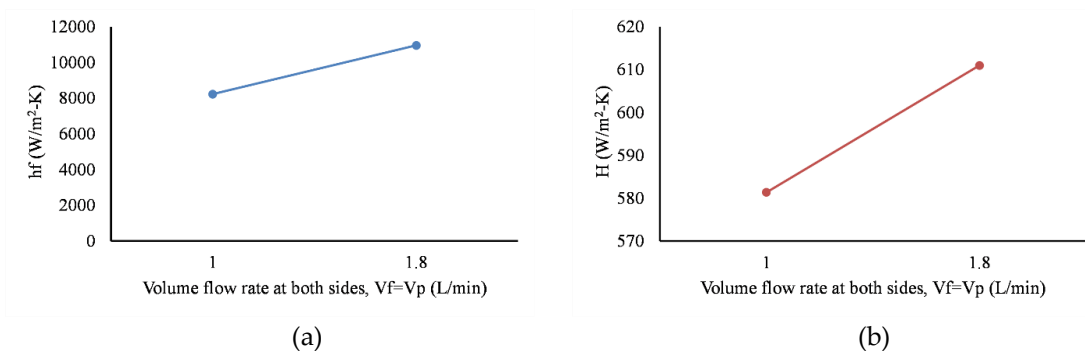


Fig. 8. The influence of volume flow rate on (a) internal heat transfer coefficient at feed side; (b) total heat transfer coefficient

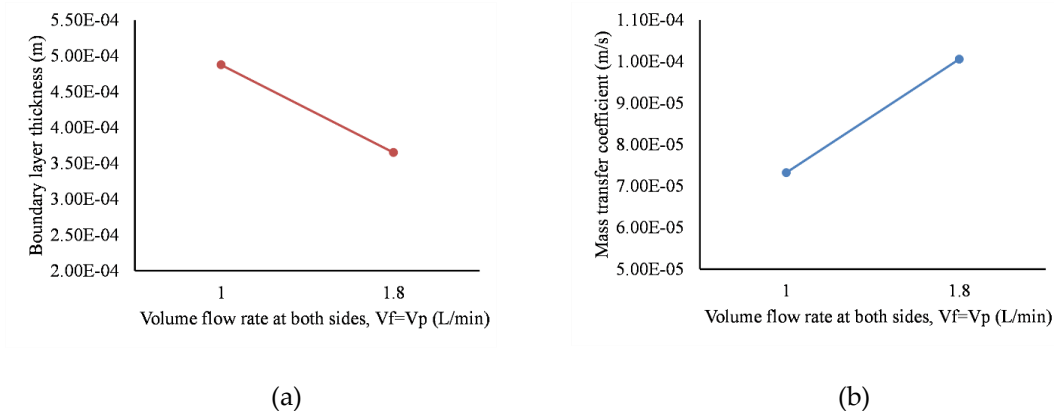


Fig. 9. The influence of volume flow rate on (a) boundary layer thickness; (b) Mass transfer coefficient through boundary layer

Effect of solution concentration on DCMD efficiency

The experimental condition was Experimental No.3 in Table 2. Under the rise in feed concentration, the permeate flux dropped insignificantly with only 1.8%, as showed in Fig. 10a. It could be attribute to the decrease in difference of partial vapor pressure between membrane surfaces, as illustrated in Fig. 10b. This behaviour was estimated by the reduction of water activity caused by the increase of mole fraction of feed solution [29, 31, 36].

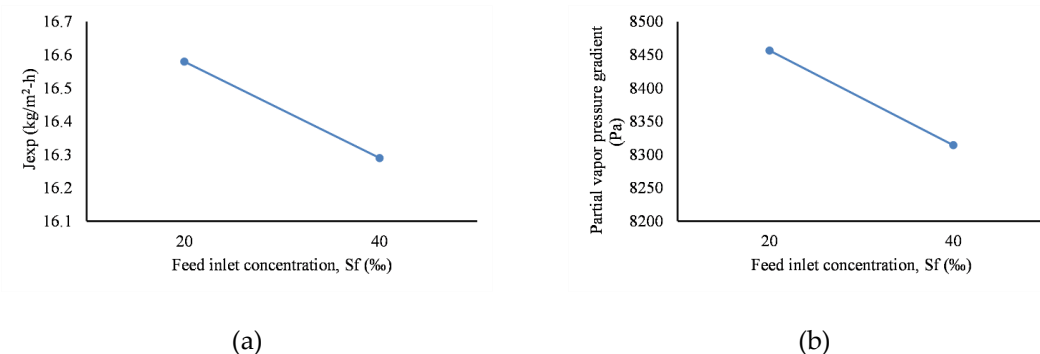


Fig. 10. The impact of feed inlet concentration on: (a) permeate flux; (b) partial vapor pressure gradient

Moreover, the slight drop in permeate flux due to the salinity could be explained through the fluctuation of boundary layer thickness and mass transfer coefficient through boundary layer. As showed in Fig 11, when the feed concentration increased from 20‰ to 40‰, there was only 1.8% rise in boundary layer thickness, and this led to 8.1% drop in mass transfer coefficient through boundary layer. Consequently, those reasons could contribute to the slight decrease in permeate flux [34].

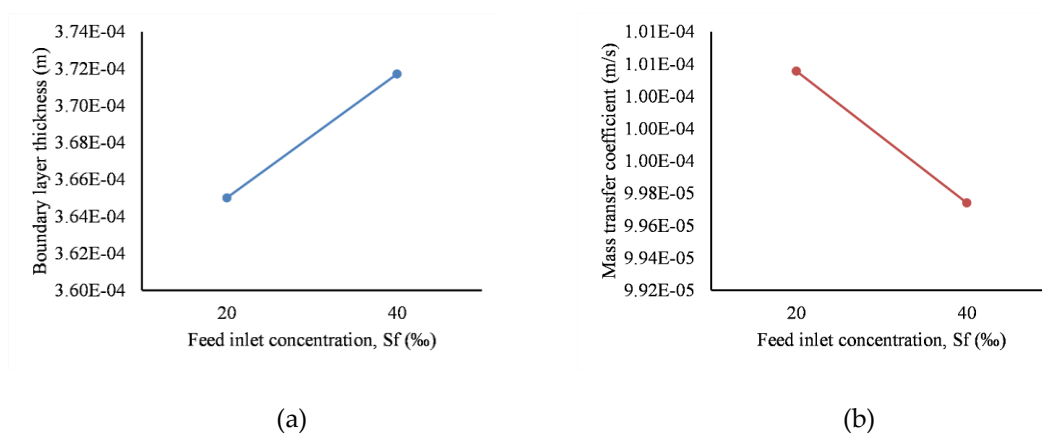


Fig. 11. The influence of feed inlet concentration on: (a) boundary layer thickness; (b) mass transfer coefficient through boundary layer

5 Conclusion

In conclusion, the salinization process happening in Quang Dien and Phu Vang district was taken into consideration. The salinization was more severely at Quang Phuoc, Quang Loi, and Phu Dien villages when 70% of water samples for irrigation purposes were brackish water. The salinity of irrigation water at Quang Thai, and Phu An villages was much lower when brackish water only accounted for 30%-40%.

The amount of freshwater produced by DCMD technology ranged from 16.3 kg/m².h to 16.6 kg/m².h when the feed concentration was in the range (40‰ – 20 ‰). Moreover, there was a considerable enhancement in freshwater production when the feed inlet temperature fluctuated from 40°C to 50°C. The salinity of collected water after DCMD treatment was under 0.1‰ which met the irrigation requirement, as mentioned in Table 1. In comparison with volume flowrate and concentration factors, feed inlet temperature was the most effective factor in enhancing the amount of freshwater production from saline water through DCMD technology.

Acknowledgment

Financial support from the project DHH2022-02-162 of Hue University is gratefully acknowledged.

Nomenclature

| | | |
|------------------|---|--|
| A | – | Membrane area, m^2 |
| C_m | – | Membrane permeability, $kg.m^{-2}.s^{-1}.Pa^{-1}$ |
| D | | Diffusion coefficient of solute, $m^2.s^{-1}$ |
| J_w | – | Experimental mass flux, $kg.m^{-2}.s^{-1}$ |
| H | – | Overall heat transfer coefficient, $W.m^{-2}.K^{-1}$ |
| $\Delta H_{v,w}$ | – | Vapour enthalpy of water, kJ/kg |
| M | – | Molecular weight of water, $kg.mol^{-1}$ |
| P_m | – | Mean pressure within the membrane pores (or total pressure), Pa |
| Q | – | The total heat flux, W |
| Q_f | – | Heat transfer rate through feed thermal boundary layer, W |
| Q_m | – | Heat transfer rate through the membrane, W |
| Q_p | – | Heat transfer rate through permeate thermal boundary layer, W |
| R | – | Gas constant, $J.mol^{-1}.K^{-1}$ |
| Re | – | Reynolds number |
| S_f | – | Feed inlet concentration, ppm |
| $S_{m,f}$ | – | Concentration on membrane surface at feed side, ppm |
| ΔT | – | The bulk temperature difference between the feed and permeate, K |
| T_f | – | Bulk feed side temperature, K |
| T_m | – | Mean temperature at membrane surface, K |
| $T_{m,f}$ | – | Temperature at the feed-membrane interface, K |
| $T_{m,p}$ | – | Temperature at the permeate-membrane interface, K |
| T_p | – | Bulk permeate side temperature, K |
| V_f | – | Volume flow rate at feed side, $L.s^{-1}$ |
| V_p | – | Volume flow rate at permeate side, $L.s^{-1}$ |

| | | |
|------------|---|--|
| d_h | – | Hydraulic diameter for spacer-filled channels, m |
| h_f | – | Heat transfer coefficient at feed side, $W.m^{-2}.K^{-1}$ |
| h_m | – | Heat transfer coefficient of the whole membrane, $W.m^{-2}.K^{-1}$ |
| h_p | – | Heat transfer coefficient at permeate side, $W.m^{-2}.K^{-1}$ |
| k_g | – | Thermal conductivity of gas phase, $W.m^{-1}.K^{-1}$ |
| k_m | – | Thermal conductivity of membrane, $W.m^{-1}.K^{-1}$ |
| k_p | – | Thermal conductivity of membrane material, $W.m^{-1}.K^{-1}$ |
| k_s | – | Mass transfer coefficient through boundary layers, $m.s^{-1}$ |
| p_a | – | Entrapped air pressure, Pa |
| $p_{v,sf}$ | – | Partial pressure of water vapour at feed-membrane surface, Pa |
| $p_{v,sp}$ | – | Partial pressure of water vapour at permeate-membrane surface, Pa |
| r | – | Mean pore size radius, m |

Greek symbols

| | | |
|-----------------|---|-------------------------------|
| τ | – | Membrane tortuosity |
| ε_m | – | Membrane porosity |
| δ_m | – | Membrane thickness, m |
| δ | – | Boundary layer thickness, m |
| ρ | – | Density of fluid, $kg.m^{-3}$ |

Subscripts

| | | |
|-----|---|----------|
| f | – | Feed |
| p | – | Permeate |

References

1. ToolBox, T.E., (2008), *Salinity of water*.
2. Health, M.o., (2009), *QCVN 01:2009/BYT National technical regulation on drinking water quality*: Ha Noi, Viet Nam.
3. Company, T.C., *Ngưỡng mặn cho nước tưới nông nghiệp và các loại cây trồng*.
4. Trường, B.T.N.v.M., (2015), *QCVN 08-MT:2015/BTNMT - Quy chuẩn kỹ thuật Quốc gia về chất lượng nước mặt*, B.T.N.v.M. trường, Editor, Bộ Tài nguyên và Môi trường: Hà Nội, Việt Nam.
5. Lê Hữu Ngọc Thanh, N.H.N., Dương Quốc Nôn, Nguyễn Thị Nhật Linh, (2018), *Nghiên cứu ảnh hưởng của xâm nhập mặn đến đất trồng lúa tại huyện Quảng Điền, tỉnh Thừa Thiên Huế*, Khoa Tài nguyên đất và Môi trường Nông nghiệp: Trường Đại học Nông Lâm, Đại học Huế.
6. Agency, V.N., (2020), *Nhiều diện tích lúa tại Thừa Thiên Huế bị chết do xâm nhập mặn*: Bộ Tài nguyên và Môi trường - Tổng cục khí tượng thủy văn.
7. Committee, Q.D.P.s., (2014), *Báo cáo tổng kết nông nghiệp năm 2014 của Phòng Nông Nghiệp và Phát Triển Nông Thôn của huyện Quảng Điền*.
8. Nguyễn Thị Hải, D.Q.N., Lê Hữu Ngọc Thanh, (2021), *Ảnh hưởng của xâm nhập mặn đến sử dụng đất trồng lúa tại xã Quảng Thái, huyện Quảng Điền, tỉnh Thừa Thiên Huế* *Tạp chí Khoa học Đại học Huế: Nông nghiệp và Phát triển nông thôn* 130, 157-167.
9. Thanh, L.H.N., (2018), *Ứng dụng GIS xây dựng bản đồ mặn đất trồng lúa tại huyện Phú Vang, tỉnh Thừa Thiên Huế*, in *Hội thảo ứng dụng GIS toàn quốc*, NXB Nông Nghiệp.
10. Ameen, N.A.M.; S.S. Ibrahim; Q.F. Alsahy; and A. Figoli, (2020), *Highly Saline Water Desalination Using Direct Contact Membrane Distillation (DCMD): Experimental and Simulation Study*. Water.
11. Cherif, H.; and J. Belhadj, (2018), *Chapter 15 - environmental life cycle analysis of water desalination processes*, in *Sustainable Desalination Handbook*, V.G. Gude, Editor, Butterworth-Heinemann. p. 527-559.
12. Karagiannis, I.C.; and P.G. Soldatos, (2008), *Water desalination cost literature: review and assessment*, *Desalination*, 223, 448-456.
13. Mezher, T.; H. Fath; Z. Abbas; and A. Khaled, (2011), *Techno-economic assessment and environmental impacts of desalination technologies*, *Desalination*, 266, 263-273.
14. Nassrullah, H.; S.F. Anis; R. Hashaikh; and N. Hilal, (2020), *Energy for desalination: a state-of-the-art review*, *Desalination*, 491, 114569.
15. Abid, M.B.; R.A. Wahab; M.A. Salam; I.A. Moujadin; and L. Gzara, (2023), *Desalination technologies, membrane distillation, and electrospinning, an overview*, *Heliyon*, 9.
16. Bamasag, A.; E. Almatrafi; T. Alqahtani; P. Phelan; M. Ullah; M. Mustakeem; M. Obaid; and N. Ghaffour, (2023), *Recent advances and future prospects in direct solar desalination systems using membrane distillation technology*, *Journal of Cleaner Production*, 385, 135737.
17. Al-Karaghoul, A.; and L.L. Kazmerski, (2013), *Energy consumption and water production cost of conventional and renewable-energy-powered desalination processes*, *Renew. Sust. Energ. Rev.*, 24, 343-356.

18. Al-Obaidani, S.; E. Curcio; F. Macedonio; G. Di Profio; H. Al-Hinai; and E. Drioli, (2008), Potential of membrane distillation in seawater desalination: thermal efficiency, sensitivity study and cost estimation, *J. Membr. Sci.*, 323, 85-98.
19. Alkaisi, A.; R. Mossad; and A. Sharifian-Barforoush, (2017), A review of the water desalination systems integrated with renewable energy, *Energy Procedia*, 110, 268-274.
20. Chafidz, A.; S. Al-Zahrani; M.N. Al-Otaibi; C.F. Hoong; T.F. Lai; and M. Prabu, (2014), Portable and integrated solar-driven desalination system using membrane distillation for arid remote areas in Saudi Arabia, *Desalination*, 345, 36-49.
21. Ashoor, B.B.; S. Mansour; A. Giwa; V. Dufour; and S.W. Hasan, (2016), Principles and applications of direct contact membrane distillation (DCMD): a comprehensive review, *Desalination*, 398, 222-246.
22. González, D.; J. Amigo; and F. Suárez, (2017), Membrane distillation: perspectives for sustainable and improved desalination, *Renew. Sust. Energ. Rev.*, 80, 238-259.
23. Lawson, K.W.; and D.R. Lloyd, (1997), Membrane distillation, *J. Membr. Sci.*, 124, 1-25.
24. Choi, Y.-J.; S. Lee; J. Koo; and S.-H. Kim, (2016), Evaluation of economic feasibility of reverse osmosis and membrane distillation hybrid system for desalination, *Desalination Water Treat.*, 57, 24662-24673.
25. Duong, H.; N. Phan; T. Nguyen; T. Pham; and N.C. Nguyen, (2017), Membrane distillation for seawater desalination applications in Vietnam: potential and challenges, *Vietnam Journal of Science and Technology*, 55.
26. Francis, L.; F. Ahmed; and N. Hilal, (2022), Advances in Membrane Distillation Module Configurations, *Membranes*, 12, 81.
27. Yalcinkaya, F., (2019), A review on advanced nanofiber technology for membrane distillation, *Journal of Engineered Fibers and Fabrics*, 14, 1558925018824901.
28. Sanmartino, J.A.; M. Khayet; M. García-Payo; N. Hankins; and R. Singh, (2016), Desalination by membrane distillation, *Emerging membrane technology for sustainable water treatment*, 77-109.
29. Alkhudhiri, A.; N. Darwish; and N. Hilal, (2012), Membrane distillation: a comprehensive review, *Desalination*, 287, 2-18.
30. Khayet, M., (2011), Membranes and theoretical modeling of membrane distillation: a review, *Adv. Colloid Interface Sci.*, 164, 56-88.
31. Khayet, M.; and T. Matsuura, (2011), *Membrane distillation: principles and applications*; Elsevier: Amsterdam, Netherlands; pp. 1-512.
32. García-Payo, M.C.; and M.A. Izquierdo-Gil, (2004), Thermal resistance technique for measuring the thermal conductivity of thin microporous membranes, *J. Phys. D Appl. Phys.*, 37, 3008-3016.
33. Ve, Q.L.; R. Koirala; M. Bawahab; H. Faqeha; M.C. Do; Q.L. Nguyen; A.S. Date; and A. Akbarzadeh, (2021), Theoretical modelling and experimental study of spacer-filled direct contact membrane distillation: Effect of membrane thermal conductivity model selection, *Desalination Water Treat.*, 217, 63-11.
34. Ve, Q.L.; R. Koirala; M. Bawahab; H. Faqeha; M.C. Do; Q.L. Nguyen; A. Date; and A. Akbarzadeh, (2021), Experimental investigation of the effect of the spacer and operating conditions on mass transfer in direct contact membrane distillation, *Desalination*, 500, 114839.
35. Qtaishat, M.; T. Matsuura; B. Kruczek; and M. Khayet, (2008), Heat and mass transfer analysis in direct contact membrane distillation, *Desalination*, 219, 272-292.

36. Schofield, R.W.; A.G. Fane; and C.J.D. Fell, (1987), Heat and mass transfer in membrane distillation, *J. Membr. Sci.*, 33, 299-313.
37. Khayet, M.; M.P. Godino; and J.I. Mengual, (2001), Modelling transport mechanism through a porous partition, *J. Non-Equil Thermody*, 26, 1.
38. Nayar, K.G.; M.H. Sharqawy; L.D. Banchik; and J.H. Lienhard V, (2016), Thermophysical properties of seawater: a review and new correlations that include pressure dependence, *Desalination*, 390, 1-24.
39. Ding, Z.; R. Ma; and A.G. Fane, (2003), A new model for mass transfer in direct contact membrane distillation, *Desalination*, 151, 217-227.
40. A Aas, G.; A. A Mea; S.M. A Ha; and A.-M. A Msa, (2017), Effect of different salts on mass transfer coefficient and inorganic fouling of TFC membranes, *J Membr Sci Technol*, 7.
41. Curcio, E.; and E. Drioli, (2005), Membrane distillation and related operations: a review, *Sep. Purif. Rev.*, 34, 35-86.
42. Schlichting, H.; and J. Kestin, (1979), *Boundary layer theory*, 7th ed ed; McGraw-Hill: New York.
43. Boudinar, M.B.; W.T. Hanbury; and S. Avlonitis, (1992), Numerical simulation and optimisation of spiral-wound modules, *Desalination*, 86, 273-290.
44. Alklaibi, A.M.; and N. Lior, (2006), Heat and mass transfer resistance analysis of membrane distillation, *J. Membr. Sci.*, 282, 362-369.
45. Bouchrit, R.; A. Boubakri; A. Hafiane; and S.A.-T. Bouguecha, (2015), Direct contact membrane distillation: capability to treat hyper-saline solution, *Desalination*, 376, 117-129.
46. Singh, D.; and K.K. Sirkar, (2014), High temperature direct contact membrane distillation based desalination using PTFE hollow fibers, *Chem. Eng. Sci.*, 116, 824-833.
47. Suleman, M.; M.B. Asif; and S.A. Jamal, (2021), Temperature and concentration polarization in membrane distillation: a technical review, *Desalination Water Treat.*